Electronic Supplementary Information (ESI):

Promotional effects of rare earth elements (Sc, Y, Ce, and Pr) on NiMgAl catalysts for dry reforming of methane

Yang Cao, Hongrui Li, Jianping Zhang, Liyi Shi and Dengsong Zhang*

Department of Chemistry, Research Center of Nano Science and Technology, Shanghai University, Shanghai 200444, P. R. China.

Fax: 86 21 66136079; E-mail: dszhang@shu.edu.cn

Supplementary data

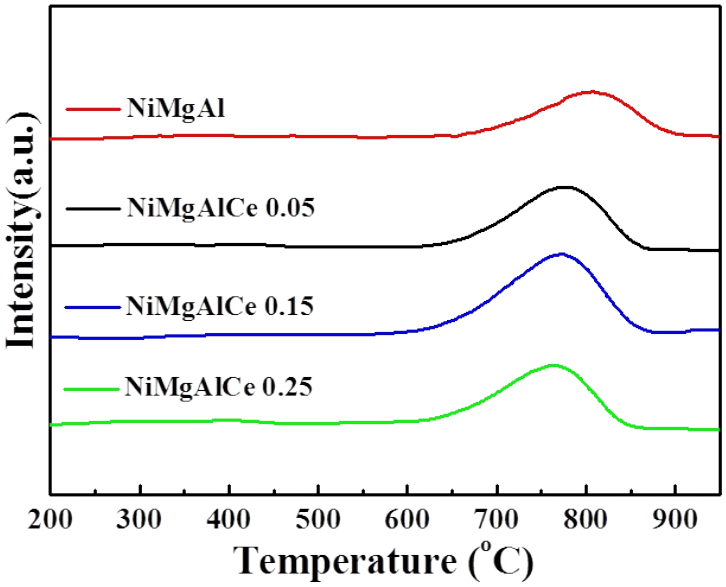

Fig. S1 H_2-TPR profiles of NiMgAlCex catalysts.

The NiMgAlCex catalysts were prepared under the same conditions except for the different amounts of cerium nitrate (0.05mmol, 0.15mmol and 0.25mmol).

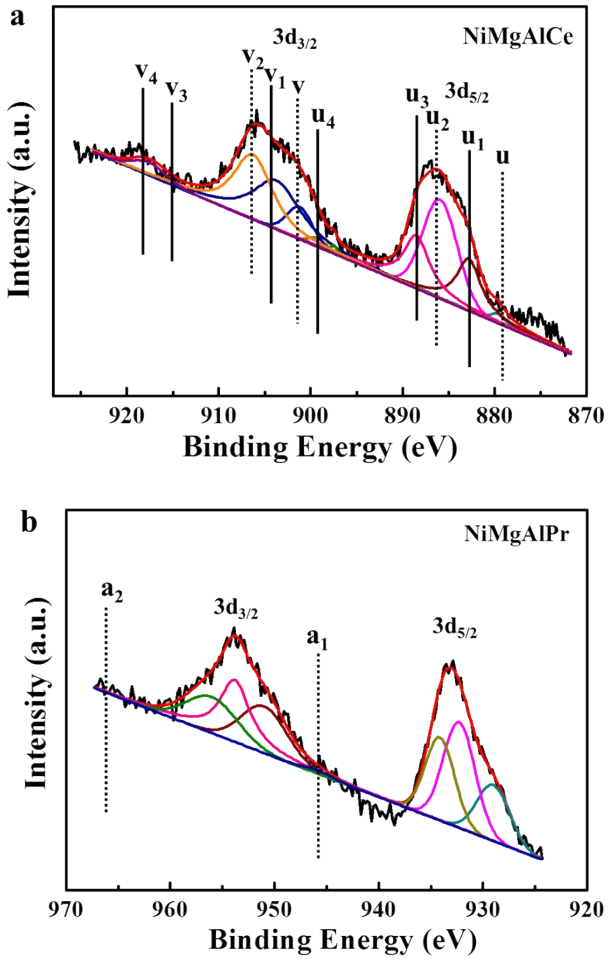

Fig. S2 (a) Ce 3d XPS spectra of NiMgAlCe catalyst; (b) Pr 3d XPS spectra of NiMgAlPr catalyst.

The Ce 3d XPS spectra of NiMgAlCe and Pr 3d XPS spectra of NiMgAlPr catalyst were shown in Figure. S2. The labels "v" and "u" represent the Ce $3d_{3/2}$ and Ce $3d_{5/2}$, respectively. The peaks referred to $u/u_2/v/v_2$ represent the presence of Ce^{3+} and the other peaks were assigned to Ce^{4+}. The estimated Ce^{3+} concentration of total Ce on the NiMgAlCe catalyst is 29.8%. As shown in Fig. S2b, two XPS peaks located at 933.5 and 953.6 eV were assigned to the Pr $3d_{5/2}$ and Pr $3d_{3/2}$, respectively. It is well-known that Pr oxides commonly coexist with Pr^{4+} and Pr^{3+}. The analysis indicated that Pr ions in the NiMgAlPr catalyst possessed dominantly the +3 valence state. However, the peaks at 946 eV (a_1) and 967 eV (a_2) were corresponds to the Pr^{4+}, suggesting the presence of Pr^{4+}.

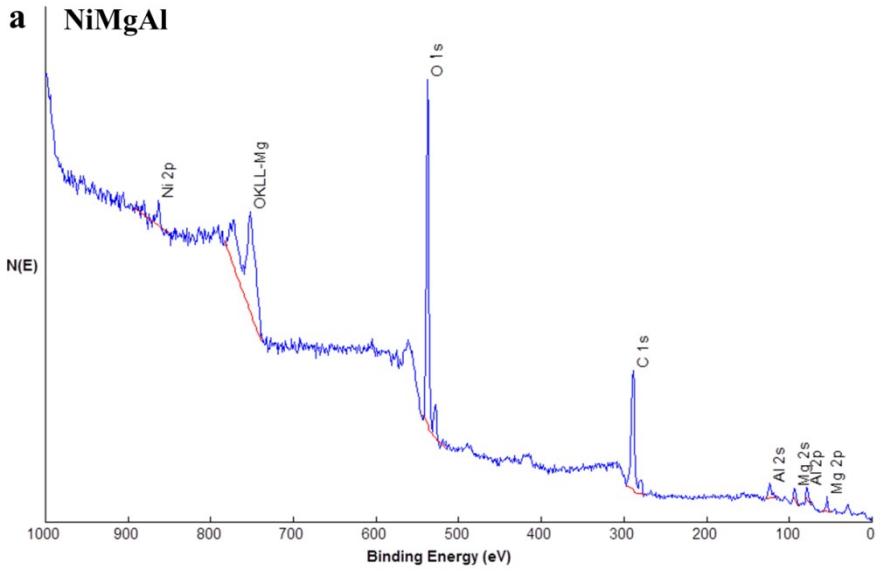
a
NiMgAl
O 1s
Ni 2p
OKLL-Mg
C 1s
Al 2s
Mg 2s
Al 2p
Mg 2p
N(E)
1000
900
800
700
600
500
400
300
200
100
0
Binding Energy (eV)

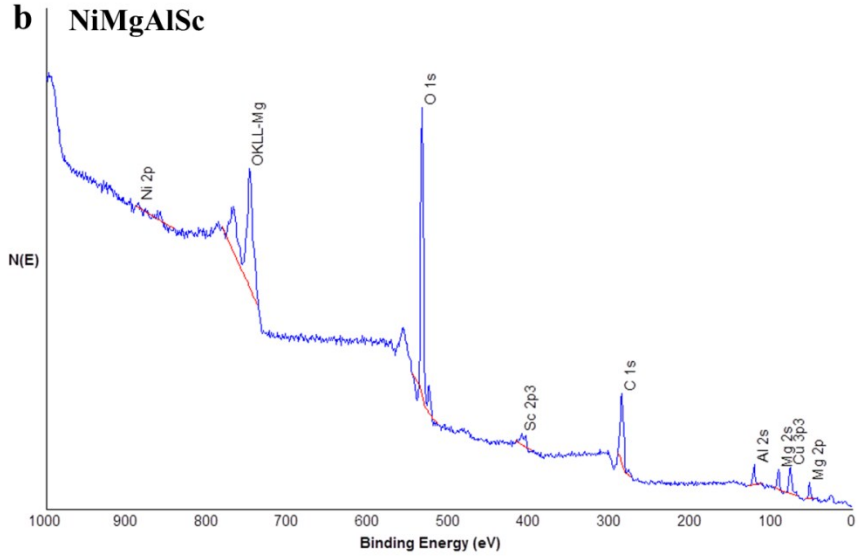
b
NiMgAlSc
O 1s
OKLL-Mg
Ni 2p
Sc 2p3
C 1s
Al 2s
Mg 2s
Cu 3p3
Mg 2p
N(E)
1000
900
800
700
600
500
400
300
200
100
0
Binding Energy (eV)

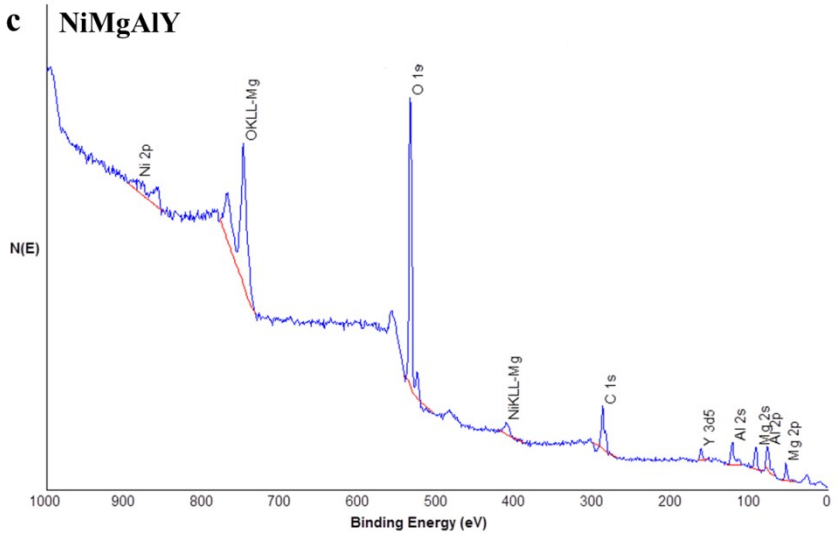
c
NiMgAlY
O 1s
OKLL-Mg
Ni 2p
NiKLL-Mg
C 1s
Y 3d5
Al 2s
Mg 2s
Al 2p
Mg 2p
N(E)
1000
900
800
700
600
500
400
300
200
100
0
Binding Energy (eV)

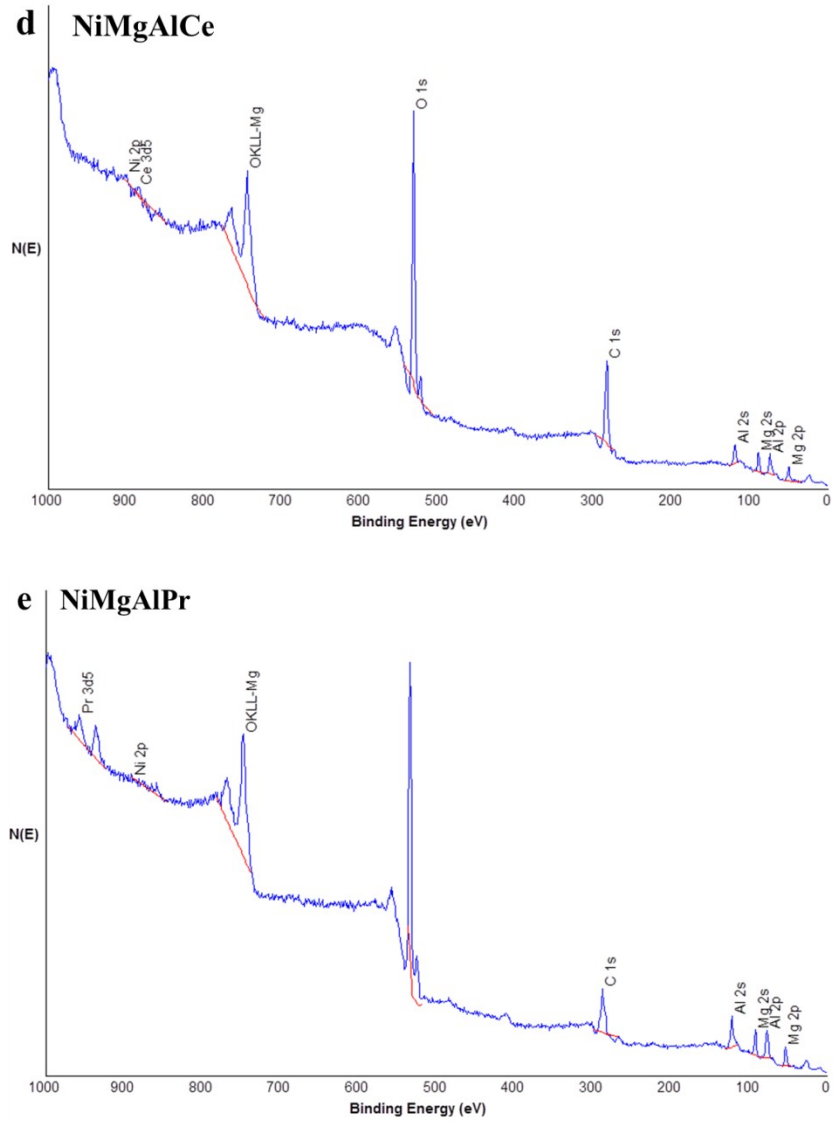

Fig. S3 XPS whole spectra of NiMgAl(RE) catalysts.

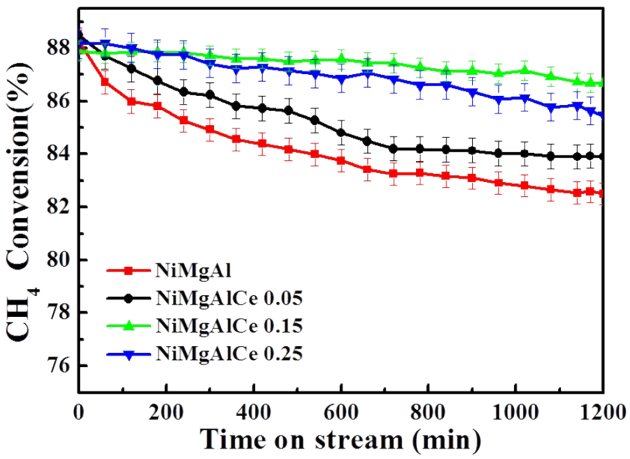

Fig. S4 The catalytic stability of NiMgAlCex catalysts.

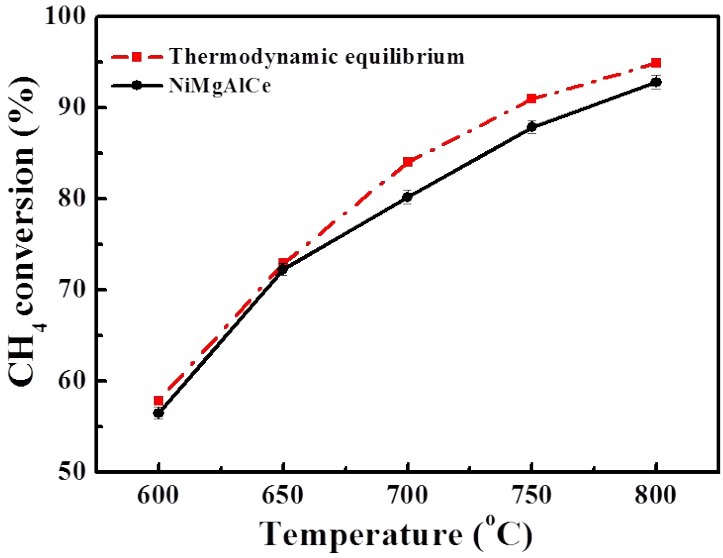

Fig. S5 DRM activity of the NiMgAlCe catalyst.

The activities of the NiMgAlCe catalyst were closer to the thermodynamic equilibrium conversions which could suggest the addition of Ce can inhibit the side reaction effectively.

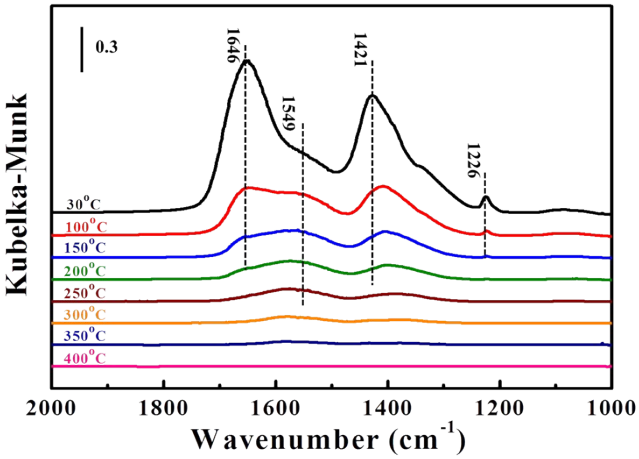

Fig. S6 *In situ* DRIFT spectra of CO_2 desorption over the NiMgAlCe catalyst as a function of time.

Table S1 Summary of the peaks in the spectra of CO_2 desorption.

Wavenumber (cm^{-1})	Assignment
1226	symmetric stretch, bidentate
1421	symmetric stretch, monodentate
1549	asymmetric stretch, monodentate
1646	asymmetric stretch, bidentate

Table S2 The conversion values of CH_4 reported in previous work

Catalysts	Temp. (°C)	Time X (h)	CH_4 conv. (%) T=0h	CH_4 conv. (%) T=Xh	References
Ni/ZrO_2	750	12	53	33	ref. 1
Ni/CeO_2	700	5	80	64	ref. 2
Ni/SiO_2–F	700	6	62	56	ref. 3
$LaNi_{0.4}Ce_{0.6}O_3$	800	10	91	80	ref. 4
$La_{0.7}Ca_{0.3}NiO_3$	750	10	78	74	ref. 5
NiMgAlCe	750	20	88	87	This work

References

1. V. M. Gonzalez-Delacruz, R. Pereñiguez, F. Ternero, J. P. Holgado and A. Caballero, ACS Catal., 2011, 1, 82-88.
2. H. Ay and D. Üner, Appl. Catal., B, 2015, 179, 128-138.
3. S. Wen, M. Liang, J. Zou, S. Wang, X. Zhu, L. Liu and Z.-j. Wang, J. Mater. Chem. A, 2015, 3, 13299-13307.
4. T. V. Sagar, N. Sreelatha, G. Hanmant, M. Surendar, N. Lingaiah, K. S. Rama Rao, C. V. V. Satyanarayana, I. A. K. Reddy and P. S. Sai Prasad, RSC Adv., 2014, 4, 50226-50232.
5. S. M. de Lima, M. A. Peña, J. L. G. Fierro and J. M. Assaf, Catalysis Letters, 2008, 124, 195-203.